Widely Tunable DS-DBR Laser With Monolithically Integrated SOA: Design and Performance

Andrew J. Ward, *Member, IEEE*, David J. Robbins, *Member, IEEE*, Giacinto Busico, Elena Barton, Lalitha Ponnampalam, Jeremy P. Duck, Neil D. Whitbread, *Member, IEEE*, Peter J. Williams, Douglas C. J. Reid, Andrew C. Carter, *Member, IEEE*, and Michael J. Wale, *Member, IEEE*

***Abstract*—We report recent device characterization results for a fully packaged widely tunable digital supermode (DS) distributed Bragg reflector (DBR) laser which has been monolithically integrated with a semiconductor optical amplifier. This new device gives all of the wide tunability and high side-mode suppression ratio performance previously reported for the DS-DBR laser with the added feature of output powers in excess of 14 dBm in fiber. In addition to output power and basic tuning behavior, we report on linewidth and relative intensity noise measurements for this device in order to investigate the noise characteristics of this laser.**

***Index Terms*—Laser tuning, semiconductor lasers, semiconductor optical amplifiers (SOAs).**

I. Introduction

IT IS NOW widely accepted that next-generation long haul communication systems will use full band tunability to make system planning as simple as possible. In addition, wide tunability is required to achieve the full potential of dynamic wavelength switching and reconfigurability—although in practice this may still be some time away. However, in order to ease the transition from fixed wavelength sources, the requirement exists for a widely tunable laser module which is a drop in replacement for a fixed wavelength DFB device in all aspects of performance, including output power, side-mode suppression ratio (SMSR), power consumption, reliability, and so on. We believe that the best approach to achieve these goals is to use a monolithic, InP, distributed Bragg reflector (DBR) platform.

To date, several designs have been proposed and demonstrated for a widely tunable DBR laser [1], [2]. Our design, the digital supermode (DS)-DBR laser, has already been described in detail elsewhere [3]–[6] but, in summary, it consists of four main sections: a rear phase grating section, which produces a comb of reflection lines; a phase control section; a multi-quantum well gain section; and a multicontact, chirped grating at the front which is used for coarse wavelength selection.

Previous results reported for the DS-DBR laser show that on its own, it does not produce a sufficiently high output power to match that of a DFB laser. This is true for all widely tunable DBR lasers which use grating sections in front of the gain section, since the optical loss associated with these extra sections limits the maximum power that can be obtained. In order to address this issue, we have integrated a low gain semiconductor optical amplifier (SOA) onto the DS-DBR laser to boost the output power by about 3–4 dB [6].

Manuscript received July 8, 2004; revised November 23, 2004.

The authors are with Bookham Inc., Caswell NN12 8EQ, U.K. (e-mail: andrew.ward@bookham.com).

Digital Object Identifier 10.1109/JSTQE.2004.841698

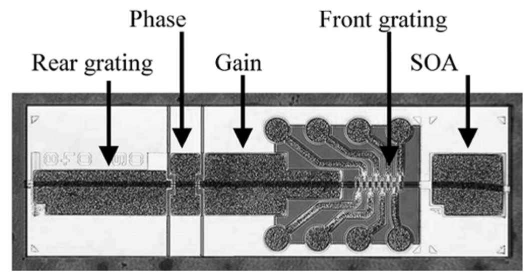

Fig. 1. Plan view photograph of a DS-DBR-SOA chip.

II. DS-DBR Design and Fabrication

As with any widely tunable DBR laser, the key elements in the DS-DBR design are its gratings. The DS-DBR laser uses two very different gratings in its design—one chirped grating at the front of the device and one phase grating at the rear. The phase grating, which has been introduced in previous letters [7], [8], consists of a number of lengths of uniform grating separated by π-phase shifts. By the correct choice of the number and positions of the phase shifts, the response of the grating can be tailored to produce a top-hat comb of reflection peaks of arbitrary number and of equal height and spacing. The design of a phase grating is best accomplished using automated optimization [7]. For the DS-DBR laser, we have used such an approach to design a phase grating with seven reflection peaks, with a 6.8-nm peak spacing. The front grating is a continuously chirped grating, 300 μm in length, over which is placed a series of short contacts for injecting current into different parts of the grating in a controlled way. This enables the enhancement of the reflection at a desired wavelength simply by injecting current into a localized part of the chirped grating, by applying current to the correct contact or contacts. The chirp rate is chosen to yield a total reflector bandwidth of around 70 nm, of which, the central 50 nm is aligned to the rear grating peaks.

The rest of the device consists of a 500-μm gain section, a 100-μm phase control section, and between the front grating and the front facet, a 350-μm SOA section. The optical waveguide is curved through the SOA section to give an output facet angle of 7°. This helps to keep unwanted facet reflection to a minimum. Fig. 1 shows a plan view of the chip where the various sections have been labeled.

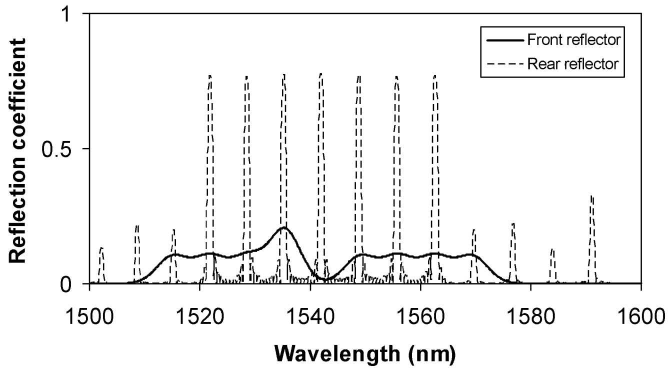

Fig. 2. Diagram showing how the current induced reflection peak in the front reflector selects one of the rear reflector peaks.

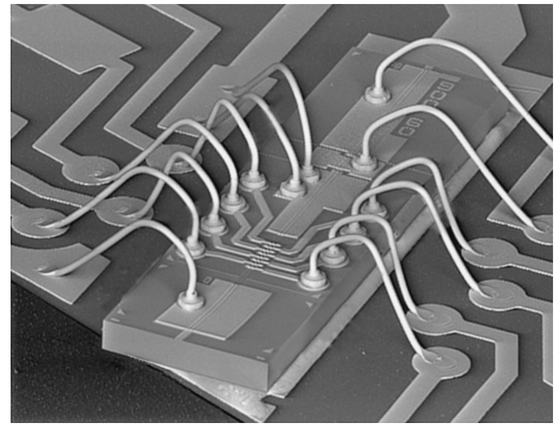

Fig. 3. SEM of a DS-DBR-SOA chip after bonding.

In operation, the front grating is used as the coarse wavelength (supermode) selection mechanism by creating a broad reflection peak which overlaps with one of the peaks from the rear phase grating comb (see Fig. 2). These sharp, rear peaks control the lasing wavelength and prevent modal competition by selecting one, and only one, of the available longitudinal modes. Fine tuning of the wavelengths of the longitudinal modes is achieved by injecting current into the phase section. In combination, this allows for continuous wavelength tuning over the full range spanned by the rear reflection comb—typically 45 nm or more. Experimentally, we have found that the correct front grating design is critical to achieving reproducible supermode control. The physical location of each front contact determines the wavelength range which is activated by that contact. The chirp rate and position of the front contacts along the chirped grating need to be carefully designed to ensure that the front peaks formed by current injection are centered on the wavelengths of the rear grating peaks. In addition, the chirped grating needs to be apodized to make the reflection response of the undriven grating as flat and featureless as possible. Without apodization, end-effects can lead to "ringing" on the grating response, which would reduce the discrimination of the reflection peaks formed by current injection.

DS-DBR devices are fabricated using standard InP processing techniques, based around a mature and stable surface ridge laser process. This process includes both holographic and e-beam grating process steps for the realization of the front and rear grating reflectors, respectively.

In brief, the process employed is as follows. The device utilizes three [metal-organo vapor phase epitaxy (MOVPE)] growth stages for, respectively; multiquantum well (MQW) source wafer growth, bulk quaternary (1.42Q) tuning section infill, and p-doped, upper confinement layer overgrowth. The gain region is defined by a dielectric mask and etch process. The infill stage uses a selective area growth approach which makes use of the dielectric mask as a nongrowth barrier. After the infill and before the overgrowth stage, front and rear gratings are written in a resist mask layer, by holographic and e-beam writes, respectively, and the pattern dry etched into the surface of a 1.15Q grating layer.

Following overgrowth, the waveguide ridge is formed by a combination of dry and wet etching. The ridge depth is determined by the material structure and is limited by an etch stop layer. The ridge width is around 2 μm. Following the deposition and definition of a dielectric isolation layer, p-contact metal is deposited and subsequently given a rapid thermal annealing (RTA) treatment in order to provide a low resistance contact. The wafer is then thinned to enable efficient chip-up and thermal heat-sinking characteristics and n-metal is deposited to form the p-i-n junction.

After the p- and n-contacts have been applied, the wafer is cleaved into bars. The lasers then have low reflectivity ($<0.2\%$) coatings deposited onto both front and rear facets.

Fig. 3 is a scanning electron microscope (SEM) image of a finished DS-DBR chip after bonding onto an alumina tile. After the devices on tile have completed testing they are transferred to an automated packaging line for building into completed modules. The results, which we will present in the rest of this paper, are obtained from these packaged devices.

III. Grating Performance

In Fig. 4, we show a comparison between the measured and modeled reflectivity of the phase grating, where the modeling was carried out using the transfer matrix approach [9], [10]. The comparison with the theoretical plot shows that we have reproduced the intended comb of seven equal peaks. Even the relative heights of the side peaks at the edges of the spectrum compare well to the predicted response.

In a similar way, Fig. 5 shows the comparison between the modeled and measured front grating response, when no currents were applied. Again, the agreement is good, showing that in the undriven state the response of the chirped grating is indeed largely flat and featureless over about 45 nm.

IV. Wavelength Tuning

The tuning performance of a typical DS-DBR-SOA device is summarized in Figs. 6 and 7. Fig. 6 shows both the (a) full wavelength tuning map and (b) a plot of wavelength as a function of rear grating current. Fig. 7 highlights the longitudinal mode structure of the device by plotting the boundaries of the modes as a function of rear and phase currents.

A wavelength tuning map [Fig. 6(a)] is a useful graphical representation of the operating response of the laser for different front and rear grating settings, with a fixed phase current (0

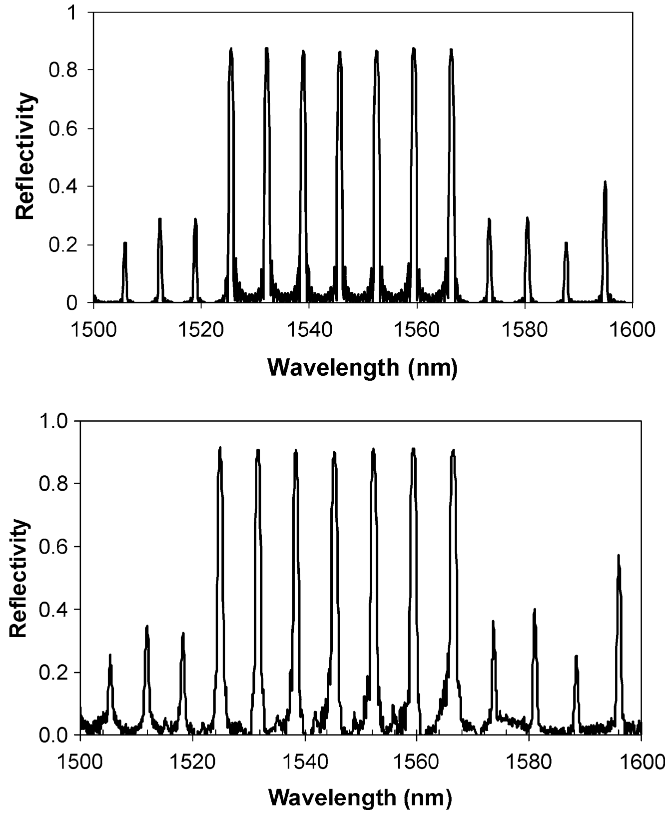

Fig. 4. Comparison of (top) modeled and (bottom) measured reflectivities for the rear phase grating.

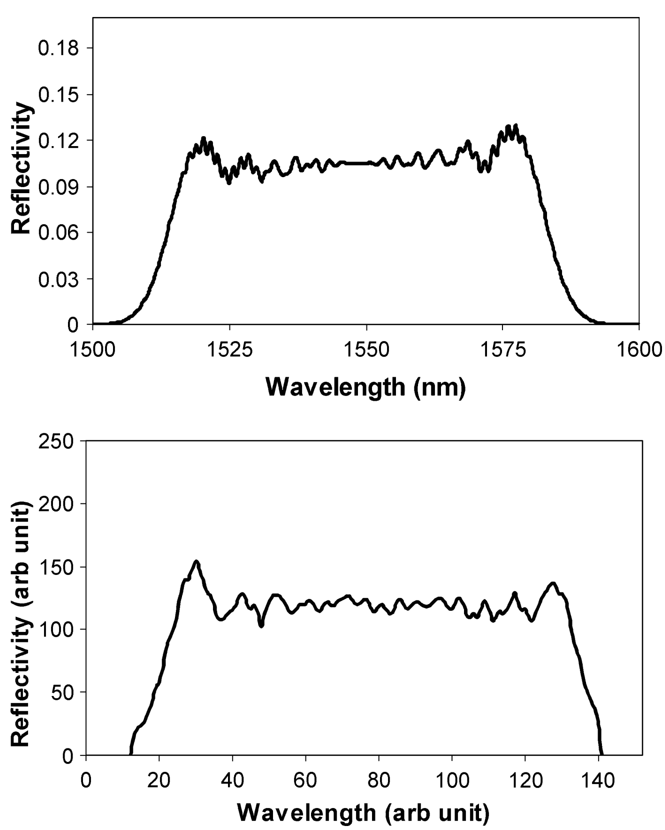

Fig. 5. Comparison of (top) modeled and (bottom) measured reflectivities for the front, apodized chirped grating.

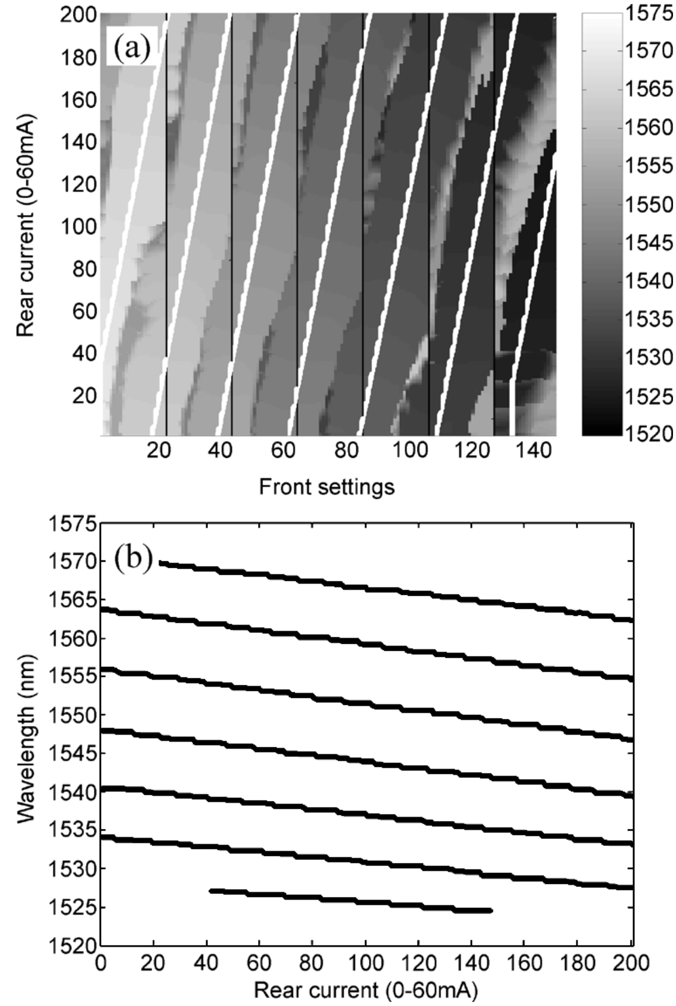

Fig. 6. Full DS-DBR tuning map (a) where the grayscale indicates the lasing wavelength obtained for different settings of the front and rear currents. This information is summarized in the line plot (b).

mA in this case). The basic principle of operation of the device is such that when current is injected into a pair of adjacent front contacts, an enhancement peak is formed in the broad front grating reflector. This allows the selection of a subband (typically ~7 nm) of the whole tuning range. The first 21 front settings along the x axis correspond to the grating contact pair 1 and 2, where the current injected into the first contact of the pair is fixed at 5 mA and the current in the second contact is ramped from 0 to 5 mA in 21 steps. The current steps are chosen in a nonlinear fashion so that smaller steps are taken at low currents where the induced refractive index changes most rapidly with current. Settings from 21 to 42 use the same scheme, but the current is now applied to gratings 2 and 3, and so on. The rear current is driven in 200 steps from 0–60 mA, again using a nonlinear pattern to account for the rapid change in index at low currents. The nonlinear axes are matched to the tuning curve and produce a linearized map at fixed phase current which is both a useful visual representation of the device tuning function and also allows easy selection of optimal trajectories for calibrating International Telecommunication Union (ITU) grid points.

The line plot [Fig. 6(b)] summarizes the wavelength information by directly plotting wavelength as a function of the rear current. In this plot, the full continuous tuning range of the device becomes apparent—about 45 nm, in this case.

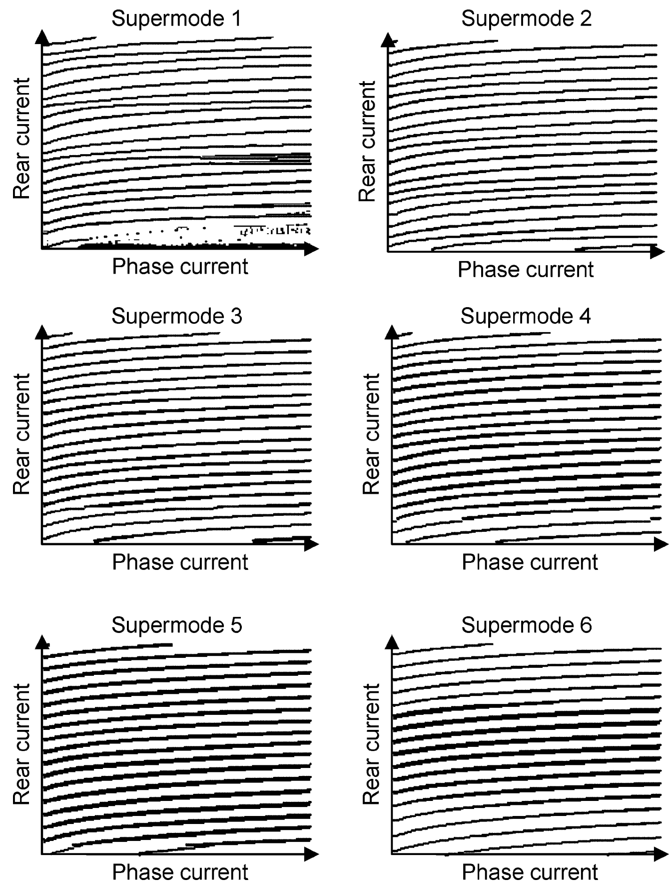

Fig. 7. Hysteresis plots which highlight the boundaries between adjacent longitudinal modes for the six complete supermodes identified in Fig. 6.

The longitudinal mode structure for the device can be explored by varying the rear and phase currents to produce a tuning map similar in structure to a three-section DBR tuning map [11]. However, at the same time as varying the rear current, we also vary the front current settings so that we track along one of the thick diagonal lines in Fig. 6(a). This helps us stay within the central region of each of the bands in the figure. We refer to these bands as the "supermodes" of the device.

In Fig. 7, we identify the boundaries between successive longitudinal modes for each supermode by plotting the hysteresis, that is, the difference in wavelength measured depending on whether the rear tuning current is being increased or decreased. All DBR lasers exhibit hysteresis to some degree and these small differences can be used to give a clear and easily obtained indication of the position of the longitudinal mode boundaries. In Fig. 7, we plot the hysteresis maps for the six of the supermodes that cover the C-band, obtained by scanning up and down in rear current. The white areas indicate regions of zero hysteresis, and the black areas show where the device is bistable and, therefore, unsuitable for ITU grid channel selection. For each map, appropriate front current settings have been used to access the different supermodes. The longitudinal modes can be seen to be even and regular and very similar in structure to those of a three-section DBR laser. This is highly advantageous since it leads to simple calibration of the device by treating each supermode as a separate three-section DBR device.

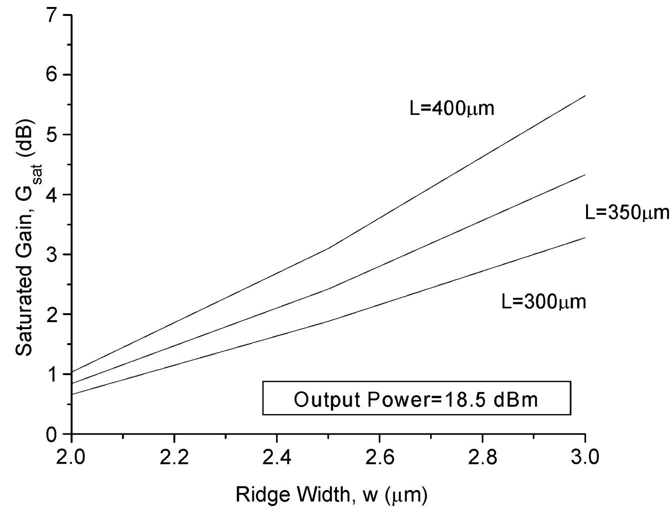

Fig. 8. Plot showing the gain achieved in the SOA model as a function of ridge width for three different amplifier lengths.

V. SOA Design Considerations

The SOA design is a tradeoff between amplification level and spectral purity—namely, SMSR and linewidth. The key to achieving these targets is to minimize the feedback from the amplifier into the laser by using a short amplifier in saturation and keeping the facet reflection low.

In order to investigate the potential effects of amplifier length and facet reflection, we have modeled both the SOA on its own and the combination of SOA and DS-DBR laser using an in-house longitudinal mode model and also the commercially available VPIcomponentMaker package from VPIsystems (a time-domain transmission-line matrix model [12]). In Fig. 8, we plot the results for the basic amplifier, showing the gain, as a function of ridge width, for a variety of possible amplifier lengths. The SMSR and linewidth calculated using the VPI package for the laser and SOA combined are shown in Fig. 9.

Together, the results show that in order to obtain 3–4 dB of amplifier gain, an SOA length of 300–400 μm is needed, coupled with a reasonably broad ridge. In terms of spectral behavior, <2-MHz linewidths can only be achieved if the facet reflection can be reduced below the 5.0×10^{-5} level for an amplifier current of 200 mA. In terms of design, this facet reflection requirement is achievable by using an angled output facet in combination with a very good broadband antireflection facet coating.

VI. Further Module Results

We now present a comprehensive set of results for one of our DS-DBR-SOA modules operated at 200-mA gain current and 150-mA SOA current. This operating point avoids complete saturation of either gain section or SOA and allows sufficient power margin for channel leveling purposes simply by reducing the SOA current. A typical power requirement specification is 13-dBm across all channels. As the gain and SOA currents are varied the output power can be plotted as a contour map, which is presented in Fig. 10. For this figure, we map the power for channel 39, which is typical of the higher power channels. As

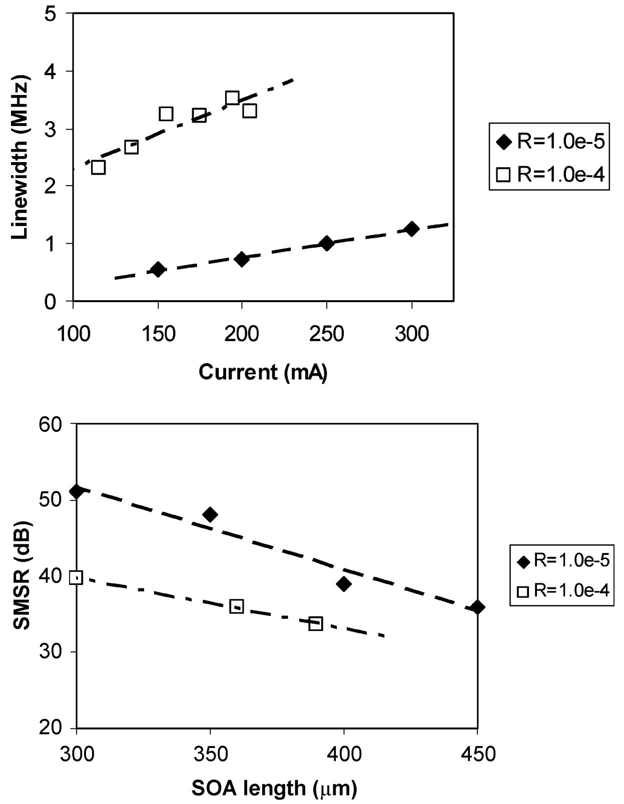

Fig. 9. Plot of time domain modeling results for the SOA showing how the linewidth (top) and SMSR (bottom) are degraded as a functions of current and SOA length, respectively. Results are given for two different facet reflectivities.

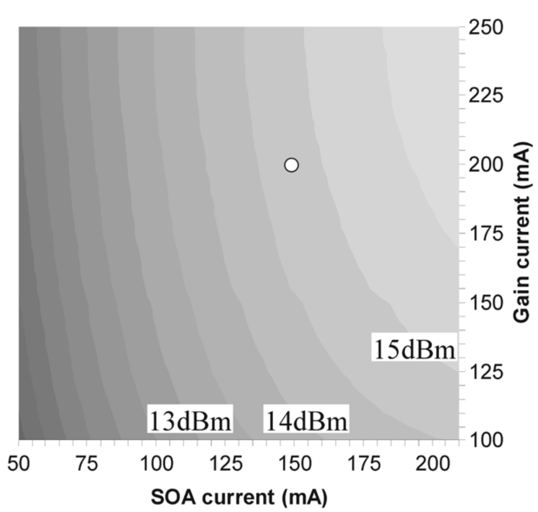

Fig. 10. Plot showing the variation in fiber coupled power with both gain and SOA currents for channel 39. Power contours are in 0.5-dB steps. The circle marks the normal operating point.

the figure shows, the technology is capable of powers in excess of 16 dBm, under suitable drive conditions.

Fig. 11 gives both the output power and SMSR measurements as a function of channel number. The device has been calibrated to operate over 119 ITU channels, where the channels are separated by 50 GHz and the first channel is 191.050 THz (1569.12 nm) and the last channel is 196.950 THz (1522.11

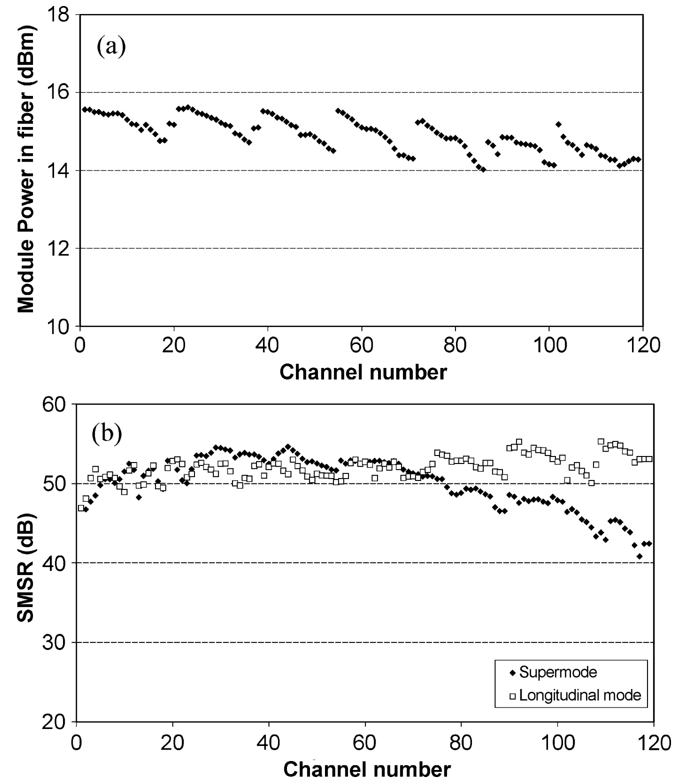

Fig. 11. Plots of measured DS-DBR-SOA module results (at 25 °C). (a) Output power in fiber. (b) SMSR.

nm). As Fig. 11(a) shows, the in-fiber output powers are in excess of 14 dBm across all channels. The supermode structure is clearly visible in the plot with the power steadily dropping within each supermode as the rear current is increased, but then jumping back to a higher value as the device is switched into the next supermode. The variation in output power across all the channels within a supermode is modest at around 1.5 dB, which is a result of both the small front tuning currents and the partial saturation of the gain of the SOA.

The spectral performance of this module is in line with modeling, with SMSR better than 40 dB in all cases, which confirms that we have achieved the low levels of facet reflection required to minimize the feedback into the laser. Analysis of the lasing spectrum (such as Fig. 12) leads to identification of two different types of mode competition. We can measure both the side-mode competition arising from adjacent longitudinal modes and also competition that arises from longitudinal modes from a different supermode. (Both the lasing mode and peaks corresponding to longitudinal modes from different supermodes can be seen in Fig. 12). These two contributions are plotted out separately in Fig. 11(b) where they are referred to as "longitudinal mode" or "supermode,'" respectively. In general, the level of longitudinal mode competition is roughly constant across the tuning range, whereas the supermode competition has a minimum at around channel 40 and increases toward both the high- and low-frequency channels, albeit rather asymmetrically. We believe that the shape of this curve follows the shape of the gain spectrum and that the supermodes close to the peak in the gain are favored relative to the supermodes on either side of the gain peak. Ultimately, it is this gain driven supermode competition that limits

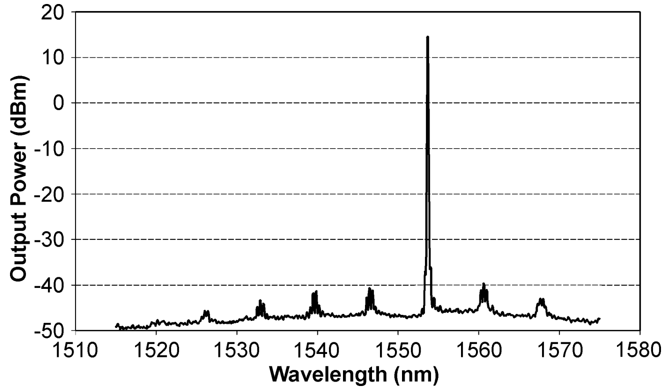

Fig. 12. Typical DS-DBR lasing spectrum. Both the lasing mode and competing modes from the other supermodes are visible.

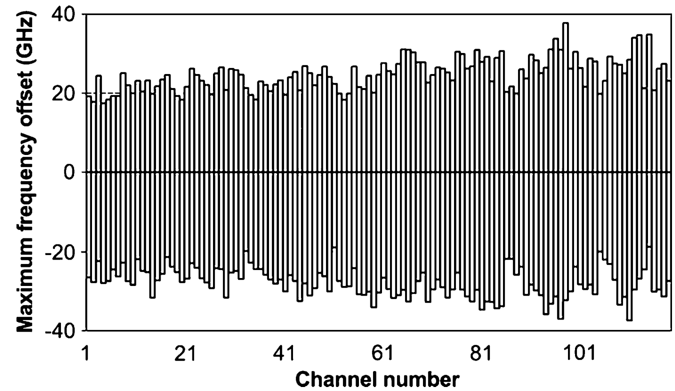

Fig. 14. Plot showing the maximum frequency deviation that can be achieved for each channel by varying only the phase current.

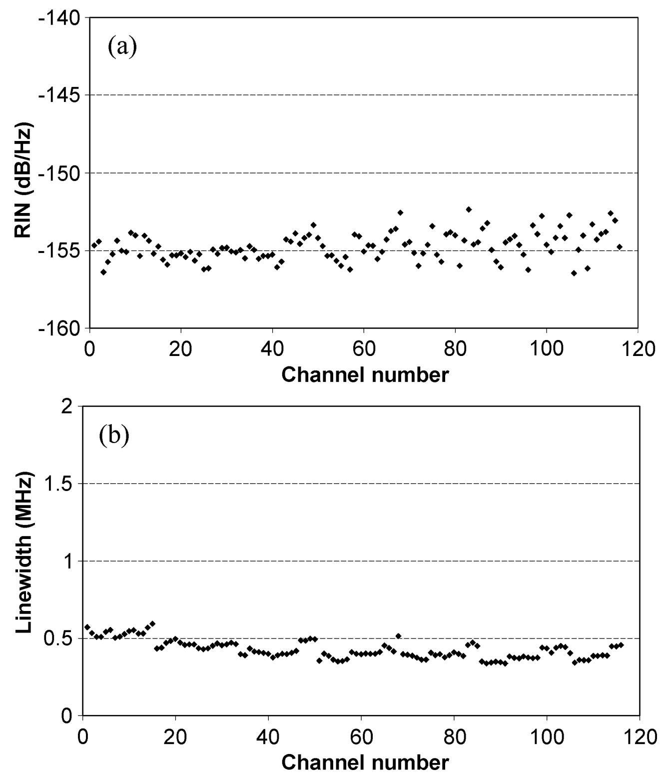

Fig. 13. Plots of measured DS-DBR-SOA module results (at 25°C). (a) RIN. (b) Linewidth.

the maximum tuning range that can be achieved. We will return to this point again in Section VII.

In Fig. 13, we plot both the relative intensity noise (RIN) and linewidth for each channel. The noise level remains low at below -150 dB/Hz across all channels and the linewidth remains below 1 MHz. For the linewidth measurements, we have followed the approach outlined in [13]. For a DBR laser, any direct measurement of linewidth usually results in a significant overestimate since it tends to be dominated by electrical noise on the current sources used to tune the laser. This noise leads to a slow dithering of the laser frequency, which in turn, manifests itself as a significant Gaussian contribution to the linewidth. However, from a transmission system point of view, it is the underlying Lorentzian linewidth which is important. We derive an estimate of the Lorentzian linewidth as follows. First, we transmit the light from the laser through an unbalanced Mach–Zehnder interferometer with 100-ps delay. The phase induced intensity noise at the output is measured with a sampling oscilloscope and an OC-192 receiver. From the measured signal-to-noise ratio the intrinsic Lorentzian linewidth can be inferred. It is this Lorentzian linewidth that is reported in Fig. 13, where the underlying supermode structure can again be seen.

In Fig. 14, we investigate the maximum frequency deviation from the calibrated channel that can be achieved by varying only the phase current before the SMSR drops below 40 dB. As the device ages, the phase current is used as part of an active control scheme to hold the channel at the correct frequency. The module includes an etalon with a free spectral range of 50 GHz to provide a stable and precise frequency reference for wavelength locking. The results of this measurement show that phase tuning can achieve at least ± 17.4 GHz of frequency control across all calibrated channels.

VII. Temperature Dependence

One important question to ask of any semiconductor laser, and of tunable lasers in particular, is their sensitivity to operating temperature. Changes in temperature affect both the refractive index of the waveguides and, hence, the effective Bragg wavelength of any gratings, and the peak wavelength of the gain spectrum. In a widely tunable laser the alignment of the grating Bragg wavelength to the peak gain wavelength can have an effect on the device performance and in particular the maximum wavelength tuning range that can be achieved.

In order to investigate this effect, a DS-DBR module was calibrated over a range of chip temperatures from 25 °C–45 °C. The resulting SMSR plots are shown in Fig. 15. These results show that the change in spectral quality with temperature is minimal with a SMSR performance of $\sim$40 dB or better across all channels, even at the highest temperature. The main effect of increased temperature is increased competition between supermodes at the high frequency end. This is attributed to the red-shift of the gain spectrum, which begins to favor the low-frequency supermodes over the high-frequency ones at elevated temperatures. This leads to a reduced SMSR (supermode contribution) at high frequency but slightly improved SMSR at low frequency. If the temperature was increased further, this would

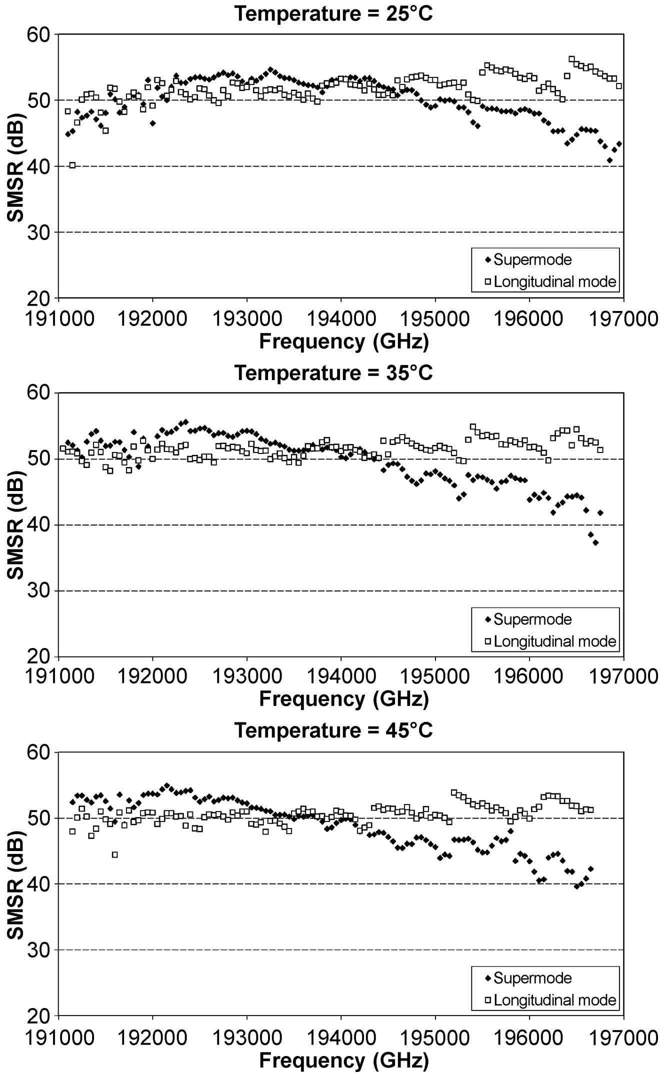

Fig. 15. Temperature dependence of the SMSR.

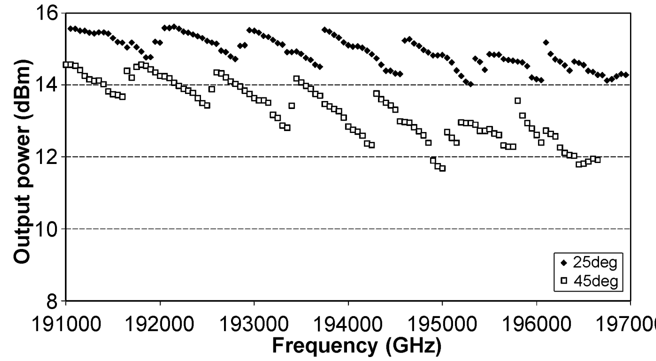

Fig. 16. Fiber coupled output power at 25 °C and 45 °C.

ultimately limit the effective tuning range as the high frequency channels would rapidly become unusable.

In addition to wavelength effects, changing the temperature also affects the output power (Fig. 16). As the temperature increases, semiconductor lasers typically suffer from increasing threshold currents and reduced efficiency which together result in lower output powers. Over the range of temperatures from 25 °C–45 °C, there is a drop in output power of 2.3 dB, comparing worst case channel at 25 °C to worst case channel at 45 °C. This corresponds to an output power of 11.7 dBm for the lowest channel at the elevated temperature.

VIII. Reliability

The DS-DBR fabrication route (Section II) utilizes the same process technology as we have already fully qualified to Telcordia-GR468 for a narrow band tunable, three-section DBR laser. We, therefore, expect full read across to the DS-DBR-SOA device and this expectation is supported by life-test data accrued to date. However, further detailed discussion lies beyond the scope of this paper.

IX. Conclusion

The DS-DBR laser monolithically integrated with an SOA gives all of the wide tunability and high SMSR performance previously reported for the DS-DBR device with the added feature of high output powers in excess of 14 dBm at 25 °C. The tuning behavior shows a series of clear three-section DBR tuning maps for the different supermodes, which makes the device easy to calibrate using automated software. Even at 45 °C, the tuning bandwidth and SMSR remain acceptable with the minimum output power only dropping to 11.7 dBm. As a result, the DS-DBR-SOA device is well positioned to challenge the incumbent, fixed wavelength DFB technology and enable future dynamic wavelength switching applications.

Acknowledgment

The authors would like to extend their thanks to all of the Fabrication Staff at Bookham, Caswell, who were involved in the manufacture of the DS-DBR devices described in this paper and, in particular, to R. A. Griffin for his guidance and assistance with the linewidth measurements. They also wish to thank the Packaging Staff at Bookham, Paignton, who assembled the devices into modules, and K Kasunic, who contributed to the early stages of the SOA design work.

References

[1] L. A. Coldren, "Monolithic tunable diode lasers," *IEEE J. Select. Topics Quantum Electron.*, vol. 6, no. 6, pp. 988–998, Nov./Dec. 2000.

[2] J. O. Wesström, G. Sarlet, S. Hammerfeldt, L. Lundqvist, P. Szabo, and P. J. Rigole, "State-of-the-art performance of widely tunable modulated grating Y-branch lasers," in *Proc. Optical Fiber Conf.*, Los Angeles, CA, 2004, Pap. TuE2, pp. 389–391.

[3] D. C. J. Reid, D. J. Robbins, A. J. Ward, N. D. Whitbread, P. J. Williams, G. Busico, A. C. Carter, A. K. Wood, N. Carr, J. C. Asplin, M. Q. Kearley, W. J. Hunt, D. R. Brambley, and J. R. Rawsthorne, "A novel broadband DBR laser for DWDM networks with simplified quasidigital wavelength selection," in *Proc. Optical Fiber Conf.*, Anaheim, CA, 2002, Pap. ThV5, pp. 541–543.

[4] A. J. Ward, D. J. Robbins, G. Busico, N. D. Whitbread, P. J. Williams, D. C. J. Reid, and J. R. Rawsthorne, "Modeling of phase-grating based wide-band tuneable lasers with simplified quasidigital wavelength selection," *IEE Proc.—Optoelectron.*, vol. 150, pp. 199–204, 2003.

[5] N. D. Whitbread, A. J. Ward, L. Ponnampalam, and D. J. Robbins, "Digital wavelength selected DBR laser," in *Proc. Photonics West, Proc. SPIE*, vol. 4995, 2003, pp. 81–93.

[6] D. J. Robbins, G. Busico, L. Ponnampalam, J. P. Duck, P. J. Williams, R. A. Griffin, A. J. Ward, D. C. J. Reid, N. D. Whitbread, E. Barton, B. Reid, and K. Kasunic, "A high power, broadband tuneable laser module based on a DS-DBR laser with integrated SOA," in *Proc. Optical Fiber Conf.*, Los Angeles, CA, 2004, Pap. TuE3, pp. 392–394.

[7] G. Sarlet, G. Morthier, R. Baets, D. J. Robbins, and D. C. J. Reid, "Optimization of multiple exposure gratings for widely tunable lasers," *IEEE Photon. Technol. Lett.*, vol. 11, no. 1, pp. 21–23, Jan. 1999.

[8] A. J. Ward, D. J. Robbins, D. C. J. Reid, N. D. Whitbread, G. Busico, P. J. Williams, J. P. Duck, D. Childs, and A. C. Carter, "Realization of phase grating comb reflectors and their application to widely tunable DBR lasers," *IEEE Photon. Technol. Lett.*, vol. 16, no. 11, pp. 2427–2429, Nov. 2004.

[9] G. Björk and O. Nilsson, "A new exact and efficient numerical matrix theory of complicated laser structures: properties of asymmetric phase-shifted DFB lasers," *IEEE J. Lightw. Technol.*, vol. 5, pp. 140–146, 1987.

[10] G. Morthier and P. Vankwikelberge, *Handbook of Distributed Feedback Laser Diodes*. Boston: Artech House, 1997.

[11] N. P. Caponio, M. Goano, I. Maio, M. Meliga, G. P. Bava, G. Destefanis, and I. Montrosset, "Analysis and design criteria of three-section DBR tunable lasers," *IEEE J. Select. Areas Commun.*, vol. 8, no. 6, pp. 1203–1213, Aug. 1990.

[12] A. Lowery, "A two-port bilateral model for semiconductor lasers," *IEEE J. Quantum Electron.*, vol. 28, no. 1, pp. 82–92, Jan. 1992.

[13] R. A. Griffin, G. Busico, J. Duck, L. Ponnampalam, D. J. Robbins, and N. D. Whitbread, "Suitability of tunable multi-section DBR lasers for advanced transmission formats," in *Proc. Eur. Conf. Optical Communication*, Rimini, Italy, 2003, Paper Th2.6.6, pp. 1012–1013.

Andrew J. Ward (M'01) received the M.A. degree from Oxford University, Oxford, U.K., and the Ph.D. degree from Imperial College, London, U.K.

In 1999, he joined GEC-Marconi, Caswell, U.K., which later became part of Bookham Inc. He is currently engaged in semiconductor laser design.

David J. Robbins (M'03) joined Bookham Inc., Caswell, U.K., in 1980, when it was part of the Plessey Company. Currently, he is a Senior Technical Specialist in R&D, working primarily on tunable DBR lasers. He has worked on the design and development of a wide range of optoelectronic and microwave devices.

Giacinto Busico received the C.Eng and Laurea degree in Ingegneria Elettronica from Ancona University, Ancona, Italy.

He spent a year researching tapered lasers at the University of Bath, Bath, U.K., and then joined Marconi, Caswell, U.K., in 2000, which is now part of Bookham Inc. His research interests included the characterization of DBR lasers.

Elena Barton, photograph and biography not available at the time of publication.

Lalitha Ponnampalam received the B.Eng. degree from University College, London, U.K., the M.S.EE. degree from School of Optics, Center for Research and Education in Optics and Lasers, University of Central Florida, Orlando, and the Ph.D. degree from Cambridge University, Cambridge, U.K.

She joined Marconi, Caswell, U.K., which later became part of Bookham Inc., as a Scientist in 2001. Her research interests include widely tunable DBR lasers.

Jeremy P. Duck received the B.Sc. and Ph.D. degrees from Sheffield University, Sheffield, U.K.

In 2000, he joined Marconi, Caswell, U.K., which is now part of Bookham Inc. Currently, he is engaged in R&D working on tunable DBR lasers.

Neil D. Whitbread (M'01) received the B.Eng. and Ph.D. degrees from the University of Sheffield, Sheffield, U.K.

He joined GEC-Marconi, Caswell, U.K., which later became part of Bookham Inc., in 1996. He is currently involved in the R&D of widely tunable semiconductor lasers and monolithic integration on InP.

Peter J. Williams received the B.Sc. and Ph.D. degrees from the University of Nottingham, Nottingham, U.K.

In 1981, he joined the Plessey Company, Caswell, U.K., which is now part of Bookham Inc. He is currently involved in the R&D of a wide range of optoelectronic devices and is working on single-frequency and tunable DBR lasers.

Douglas C. J. Reid received the B.Sc. and M.Sc. degrees from Imperial College, London, U.K.

In 1968, he joined the Plessey Company, Caswell, U.K., which is now part of Bookham Inc. His research interests have included holographic data storage, fiber gratings, and wafer gratings for semiconductor lasers.

Andrew C. Carter (M'99) received the M.A. and D.Phil. degrees from Oxford University, Oxford, U.K.

He is currently Vice President of R&D with Bookham Inc., Caswell, U.K. He has particular repsonsibility for the III-V Chip R&D.

Michael J. Wale (M'92) received the M.A. and D.Phil. degrees from Oxford University, Oxford, U.K.

He is currently the Director of Active Products Research at Bookham Inc., Caswell, U.K. Since 1982, he has been engaged in research and development of optoelectronic device technology and systems applications.